Flexible Supercapacitors

International Edition: DOI: 10.1002/anie.201603417
German Edition: DOI: 10.1002/ange.201603417

Strong and Robust Polyaniline-Based Supramolecular Hydrogels for Flexible Supercapacitors

*Wanwan Li, Fengxian Gao, Xiaoqian Wang, Ning Zhang, and Mingming Ma**

Abstract: *We report a supramolecular strategy to prepare conductive hydrogels with outstanding mechanical and electrochemical properties, which are utilized for flexible solid-state supercapacitors (SCs) with high performance. The supramolecular assembly of polyaniline and polyvinyl alcohol through dynamic boronate bond yields the polyaniline–polyvinyl alcohol hydrogel (PPH), which shows remarkable tensile strength (5.3 MPa) and electrochemical capacitance (928 $F g^{-1}$). The flexible solid-state supercapacitor based on PPH provides a large capacitance (306 $mF cm^{-2}$ and 153 $F g^{-1}$) and a high energy density of 13.6 $Wh kg^{-1}$, superior to other flexible supercapacitors. The robustness of the PPH-based supercapacitor is demonstrated by the 100% capacitance retention after 1000 mechanical folding cycles, and the 90% capacitance retention after 1000 galvanostatic charge–discharge cycles. The high activity and robustness enable the PPH-based supercapacitor as a promising power device for flexible electronics.*

Mechanically flexible power devices with large capacity, high stability and good mechanical properties are needed for powering flexible electronics devices.[1] Various flexible supercapacitors (SCs) have been designed to provide high power density, modest energy density, fast charge–discharge capability, and long cycle life.[2] Current flexible supercapacitor electrodes are generally made of electroactive carbon-based materials,[3] metal oxides,[4] conductive polymers,[5] and the composites of these materials.[6] To achieve flexible supercapacitor electrodes that can sustain a large mechanical strain, these electroactive materials are coated as a thin layer onto elastic but electrochemically non-active substrates, such as rubber fibers,[7] polydimethylsiloxane films,[8] and cotton sheets.[9] These non-active substrates occupy a significant amount of weight and volume in the final supercapacitor devices, which is not favorable for flexible electronic devices.[10] In contrast, conductive polymer-based hydrogels (CPHs) can sustain a large mechanical deformation by themselves. A few CPHs based on PEDOT-PSS,[11] polyaniline,[12] and polypyrrole[13] have been studied for flexible supercapacitors development. However, most of current CPHs are mechanically weak, with a tensile strength typically less than 1 MPa.[14] The electrochemical and mechanical stability of current CPHs also needs to be improved.[15] Therefore, strong and robust CPHs are highly desired for high-performance flexible supercapacitors, but remain as a challenge.

Inspired by the dynamic network structure of animal dermis, in which collagen fibril (rigid and strong) and elastin fibril (soft and elastic) crosslink through supramolecular interactions to form a sturdy and flexible material,[16] we hypothesized that the combination of a rigid conductive polymer with a soft hydrophilic polymer through proper supramolecular interactions would yield a strong and robust CPH.[17] We chose polyvinyl alcohol (PVA) as the soft polymer, and polyaniline (PANI) as the rigid polymer. Since boric acid can cause gelation of PVA solution to give a robust gel,[18] and boronic acid groups can be covalently incorporated onto PANI by copolymerization of 3-aminophenylboronic acid (ABA) and aniline (AN),[19] we chose boronic acid as the functional group to crosslink PVA and PANI at molecular level to form polyaniline-polyvinyl alcohol hydrogel (PPH). Several CPHs based on PANI and PVA have been reported, which were made from either physical blending of PANI particles and PVA solution with subsequent crosslinking,[20] or by impregnation of aniline into preformed PVA hydrogel with subsequent polymerization of aniline.[12c,21] These CPHs were studied for biomedical applications, whose electrochemical and mechanical properties are not suitable for supercapacitors.[20–22] Wei and co-workers used a chemically crosslinked PVA-H_2SO_4 hydrogel as substrate and electrolyte, which was coated by two thin layers of PANI to form a flexible supercapacitor.[12c] In contrast, our PPH was prepared by supramolecular assembly of PANI and PVA at molecular level, which showed remarkable mechanical and electrochemical properties. A flexible solid-state supercapacitor was fabricated based on PPH, which provided a large electrochemical capacitance (306 $mF cm^{-2}$ and 153 $F g^{-1}$) and a high energy density of 13.6 $Wh kg^{-1}$, superior to other flexible supercapacitors. The robustness of the PPH-based supercapacitor was demonstrated by the 100% capacitance retention after 1000 mechanical folding cycles, and the 90% capacitance retention after 1000 galvanostatic charge–discharge cycles.

As shown in Figure 1a, when the oxidant ammonium persulfate (APS) was added into the colorless solution of PVA, AN, and ABA, a dark green hydrogel formed quickly at room temperature (Figure 1b left). AN and ABA were copolymerized to form PANI bearing boronic acid groups. The intermolecular interaction between boronic acid groups on PANI and hydroxy groups on PVA serves as the crosslink

[*] W. Li, F. Gao, X. Wang, Dr. N. Zhang, Prof. Dr. M. Ma
CAS Key Laboratory of Soft Matter Chemistry, iChEM (Collaborative Innovation Center of Chemistry for Energy Materials), Department of Chemistry, University of Science and Technology of China
Hefei, Anhui 230026 (P.R. China)
E-mail: mma@ustc.edu.cn
Homepage: http://staff.ustc.edu.cn/~mma/
Supporting information and the ORCID identification number(s) for the author(s) of this article can be found under http://dx.doi.org/10.1002/anie.201603417.

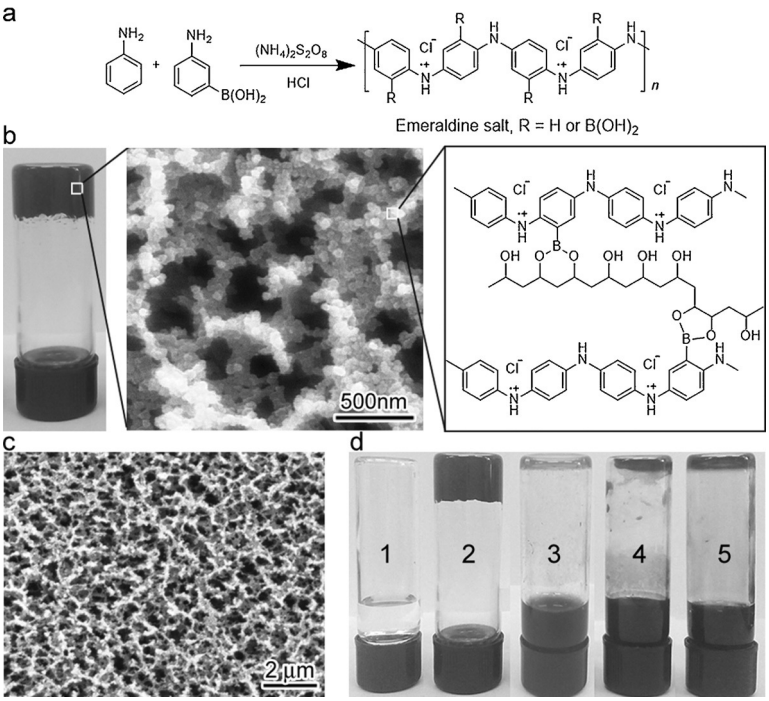

Figure 1. a) Synthesis of polyaniline bearing boronic acid groups. b) PPH at three length-scales. left: a photograph of PPH; middle: a SEM image of PPH; right: a schematic molecular structure of PPH showing the crosslink between PANI and PVA. c) SEM image of PPH showing the porous structure. d) Photographs of the reactions with different combinations of reagents. Vial 2 has all the four reactants and gives PPH. Vial 1 has no APS; vial 3 has no PVA; vial 4 has no ABA; vial 5 has no AN.

between rigid PANI and flexible PVA chains, leading to a rapid gelation. Notably, all the four reagents (APS, PVA, AN, and ABA) were required for the gelation. As shown in Figure 1d, if any one of the four reagents is missing, no gelation occurs. With all the four reagents present, the PPH can be facilely synthesized in a wide range of reaction conditions. Among these variable conditions, the most important one is the ABA:AN molar ratio, which determines the density of boronic acid group on PANI chains. When the ABA:AN molar ratio is lower than 0.03:1, no hydrogel forms, likely due to the insufficient crosslink between PANI and PVA. The optimized ABA:AN molar ratio was found to be 0.07:1 (Supporting Information and Table S1). After purification through extensive washing by deionized (DI) water, the obtained PPH sample was stored in DI water. The water content of the fully hydrated PPH sample was determined to be 70 wt % by thermogravimetry (Figure S1 in the Supporting Information), and also confirmed by lyophilization method.

Based on the comparison of infrared (IR) spectrum of PVA, PANI and PPH (Figure S2), the peaks at 1572 and 1491 cm^{-1} in the IR spectrum of PPH were assigned to the benzene ring vibration of PANI,[23] and the peaks at 3224, 2906, and 1051 cm^{-1} were attributed to the vibrations of O–H, C–H, and C–O bonds of PVA,[24] respectively, indicating the presence of both PANI and PVA in PPH. The UV/Vis spectrum of PPH suspension (Figure S3) shows a band at 430 nm and a long tail up to 800 nm, assigned to the polaron/bipolaron transition of the protonated PANI, which are the features of conductive PANI.[23] Scanning electron microscopy image of PPH (Figure 1c) shows a porous network structure, which is consisted by interconnected globular nanoparticles with a diameter around 50 nm (Figure 1b middle). The nitrogen adsorption–desorption isotherm curve (Figure S4a) shows a typical type IV isotherm with a narrow hysteresis loop, indicating a porous microstructure with open-pores. The Brunauer–Emmett–Teller (BET) specific surface area of the dehydrated PPH is 90.2 $m^2 g^{-1}$, which is 2-fold higher than other PANI based nanomaterials.[25] The pore size distribution curve (Figure S4b) shows peaks around 10, 25, and 90 nm, indicating the mesoporous feature of PPH, which would facilitate mass transfer within PPH. Indeed, the conductivity of hydrated PPH was measured to be approximately 0.1 $S cm^{-1}$ at room temperature (Figure S5), which is much higher than most of other CPHs (typically in the range of 10^{-4}–10^{-2} $S cm^{-1}$).[26] The XRD pattern of dehydrated PPH (Figure S6) shows two narrow peaks at 20° and 41° assigned to PVA,[27] and one peak around 25° corresponding to PANI,[23] indicating that PPH possesses a partially ordered structure at nanometer scale.

As shown in Figure 2a, the PPH is mechanically robust, which can be made into a knot and stretched. The PPH (water content 70 wt %) shows a typical tensile stress–strain curve for hard elastic polymer (such as polypropylene),[28] with a Young's modulus of 27.9 MPa, a tensile strength of 5.3 MPa and an elongation at break of 250 % (Figure 2b). The PPH behaves like rubber, which can be repeatedly stretched or compressed, and recover immediately to its original shape and size after being released (Movie S1,S2). Upon compres-

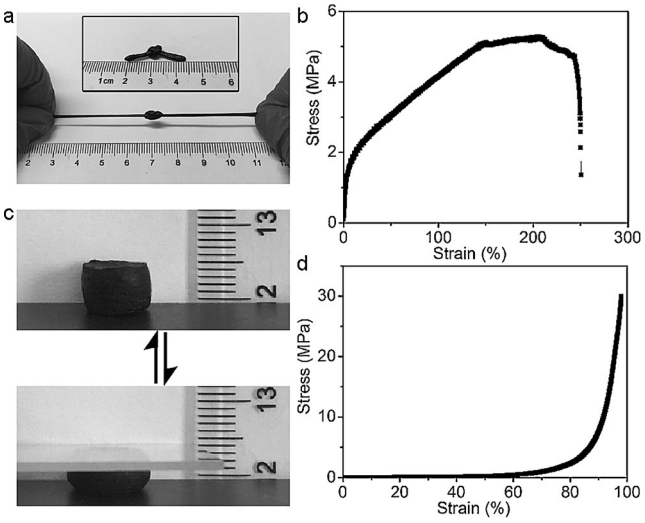

Figure 2. Mechanical properties of PPH. a) Photographs of a PPH knot upon stretching. b) The tensile stress–strain curve. c) Photographs of a PPH sample upon repeated compression. d) The compression stress–stain curve.

sion, no water is squeezed out the PPH (Figure 2c, Movie S1), indicating that PPH is a stable hydrogel, rather than a sponge. The PPH can be compressed to 98% strain without being broken, with a compressive stress of 30 MPa (Figure 2d). These mechanical metric values clearly demonstrate that PPH is a very strong and robust hydrogel, comparable to other strong hydrogels, such as topological gels,[29] nanocomposite gels,[30] double-network gels,[31] tetra-arm polyethylene glycol gels,[32] ionic gels,[33] and microsphere composite gels.[34]

To probe the supramolecular structure of PPH, a PPH film was incubated in 80 °C water for 12 h to hydrolyze the boronate bonds between PVA and PANI. The substance dissolved in hot water was lyophilized and identified as PVA by IR (Figure S7a). The remaining film showed an IR spectrum similar to that of PANI, while the characteristic peaks of PVA in 2900–3300 cm^{-1} region disappeared (Figure S7b). This result suggests that most of PVA in PPH was dissolved into hot water, with PANI left insoluble, which indicates the supramolecular nature of PPH. The remaining film became much weaker (tensile strength 0.4 MPa, elongation at break 40%, Figure S8) than the original PPH film, implying the key role of PVA for the superior mechanical properties of PPH.

To examine the electrochemical properties of PPH, a PPH electrode was made by in situ gelation of PPH on a piece of hydrophilic carbon cloth that serves as a flexible current collector. The PPH electrode was characterized by using cyclic voltammetry (CV), electrochemical impedance spectroscopy (EIS) and galvanostatic charge–discharge (GCD) methods, in a three-electrode system with 1M H_2SO_4 as the electrolyte. To explore the scope of the PPH electrode, we varied the areal loading of PANI from 0.5 mg cm^{-2} to 4 mg cm^{-2}, and examined the obtained PPH electrodes by using GCD method at a current density of 1 Ag^{-1}. As shown in Figure 3a, the highest specific capacitance was obtained with 0.5 mg cm^{-2} PANI loading, reaching 1350 F g^{-1} based on the mass of PANI, which is much higher than previously reported conductive polymer based electrodes (typically in the range of 200–800 F g^{-1}, Table S2). The highest areal capacitance was obtained with 4 mg cm^{-2} PANI loading, reaching 2320 mF cm^{-2}, which is also several folds higher than other PANI-based electrodes (typically in the range of 100–500 mF cm^{-2}).[12c] As a control, the bare hydrophilic carbon cloth was tested by CV, which showed a negligible areal capacitance (37.8 mF cm^{-2}, Figure S9) in comparison to that of the PPH electrode. When the PANI loading increased, the specific capacitance of PPH electrode gradually decreased, while the areal capacitance gradually increased. At 2 mg cm^{-2} PANI loading, the requests for both high specific capacitance and high areal capacitance were balanced. Therefore, the PANI loading of PPH electrode was fixed at 2 mg cm^{-2} for the following tests.####

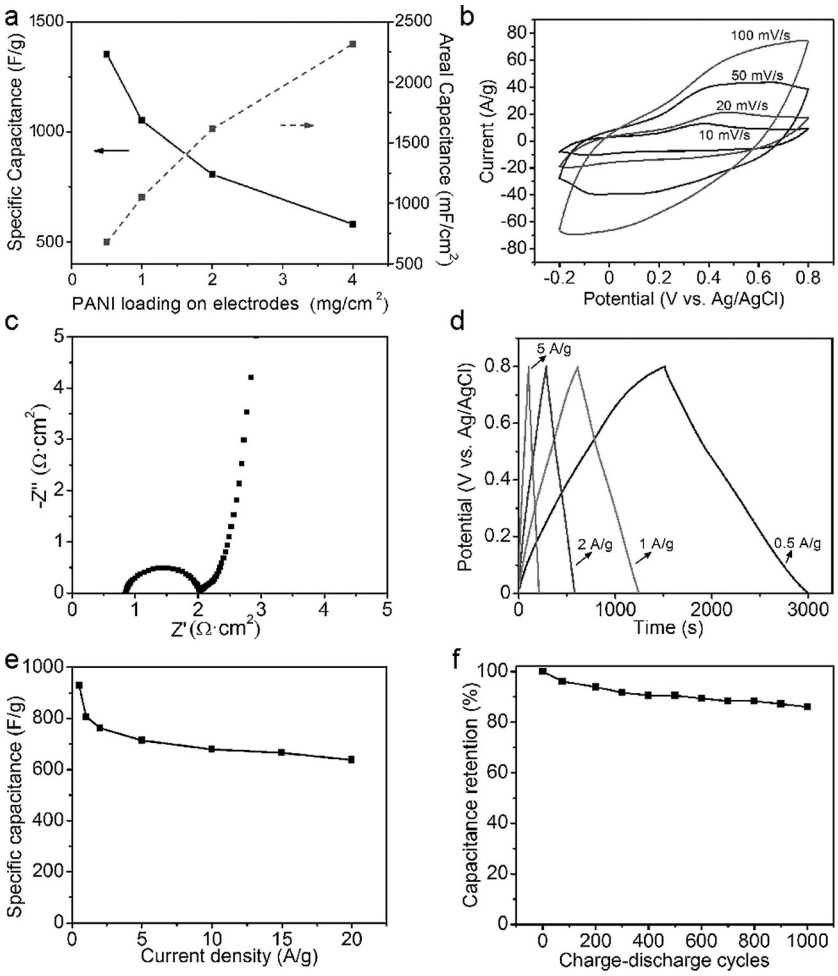

Figure 3. a) Specific capacitance and areal capacitance of PPH electrodes with different PANI loading. Data in b)–f) are based on a PPH electrode with 2 mg cm^{-2} PANI loading. b) CV diagrams at scan rates of 10–100 mV s^{-1}. c) Impedance plot in the frequency range of 0.01 Hz to 100 kHz. d) GCD curves at current densities of 0.5–5 A g^{-1}. e) Specific capacitance of the PPH electrode at varied GCD current densities. f) Capacitance retention during GCD cyclic test at a current density of 20 A g^{-1}.

As shown in Figure 3b, characteristic redox peaks of PANI are observed on the CV traces, indicating the transformation between different redox status of PANI.[35] The electrochemical kinetics and ionic resistance were studied by EIS (Figure 3c). The slope of the EIS plot in the low frequency region is close to 90°, indicating a good capacitive behavior.[12a] In the high frequency region, R_Ω is 0.86 Ω cm^{-2}, indicating a small series resistance. The semicircle on the EIS plot shows a small charge-transfer resistance (1.15 Ω cm^{-2}), indicating a favorable charge-transfer kinetics for the PPH electrode.[36] Figure 3d shows symmetrical GCD curves of the PPH electrode, indicating highly reversible charge–discharge behavior. The iR drops (the voltage drops due to resistance) on these GCD curves are negligible, owing to the high conductivity of PPH and the carbon cloth. The specific

capacitance of PPH electrode was calculated based on the GCD data (Figure 3d and Figure S10). The capacitance of PPH electrode measured at 0.5 $A g^{-1}$ reaches 928 $F g^{-1}$ and 1856 $mF cm^{-2}$, which are much higher than that of previously reported conductive-polymer-based electrodes (Table S2). The PPH electrode shows a good rate performance, with 84% capacitance retention when current density was increased from 1 $A g^{-1}$ (806 $F g^{-1}$) to 10 $A g^{-1}$ (678 $F g^{-1}$). The rate performance is also much better than reported conductive-polymer-based electrodes, which typically give 50–60% capacitance retention at a 10-fold higher current density.[37] As shown in Figure 3f, the PPH electrode is electrochemically stable, with 86% capacitance retention after 1000 GCD cycles at a current density of 20 $A g^{-1}$. In addition, the Coulombic efficiency of PPH electrode remains close to 100% during the long-term GCD cyclic test (Figure S11). Conductive polymers usually suffer poor cyclic stability caused by the swelling and shrinking during the charge–discharge process.[38] The good electrochemical stability of PPH electrode should be attributed to the strong and elastic mechanical properties of the PPH, resulting in a supportive and protective effect on PANI during swelling and shrinking.

To examine the practical application of the PPH electrode for flexible supercapacitors, a symmetric solid-state supercapacitor device was fabricated by sandwiching two PPH electrodes and a polyester mesh as the separator, and PVA–H_2SO_4 gel as the electrolyte (Figure 4a, see Supporting Information for details). This PPH-based supercapacitor was tested by using CV, EIS, and GCD methods in a two-electrode system. The CV diagrams at different scan rates (Figure 4b) present similar and symmetric shape, suggesting good capacitive behavior of this supercapacitor. The small charge-transfer resistance in the EIS plot (Figure 4c and inset) indicates a favorable electrochemical kinetics of this supercapacitor. Also, the vertical tail in the EIS plot also implies a good capacitive character of this supercapacitor.[12a] GCD curves (Figure 4d) show a typical charge-discharge pattern for PANI-based supercapacitors.[39] The specific capacitance of this supercapacitor was calculated based on the total mass of PANI in this device (Figure 4e). This supercapacitor demonstrates both a high areal capacitance of 306 $mF cm^{-2}$ (Figure S12) and a high specific capacitance of 153 $F g^{-1}$ at a discharge rate of 0.25 $A g^{-1}$.This supercapacitor also shows a very good rate performance, with 87% capacitance retention when the current density was increased from 0.25 $A g^{-1}$ (153 F g^{-1}) to 2.5 $A g^{-1}$ (133 $F g^{-1}$), superior to the performance of other flexible supercapacitors.[40] As shown in Figure 4f, this supercapacitor provides a good electrochemical stability, with 90% capacitance retention after 1000 GCD cycles at a current density of 2.5 $A g^{-1}$. The capacitance and stability of this PPH-based supercapacitor are superior to other flexible supercapacitors (see Table S3). The Coulombic efficiency of this supercapacitor remains close to 100% during the long-term GCD cyclic test (Figure S13). In addition, this supercapacitor exhibits a high energy density of 13.6 $Wh kg^{-1}$ at a power density of 105 $W kg^{-1}$ for a 0.8 V voltage window (Figure S14), which is among the best of current flexible supercapacitors.[40]

Owing to the outstanding mechanical properties of PPH, this supercapacitor can be deformed repeatedly, which does

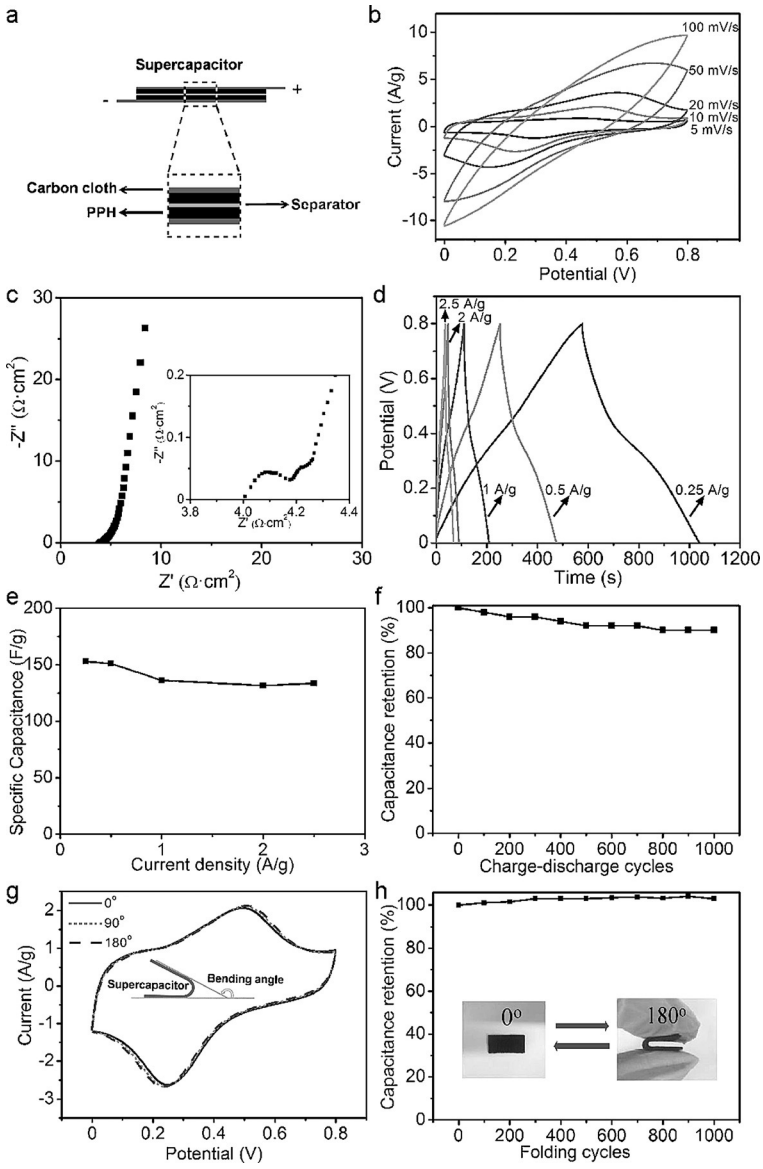

Figure 4. a) Schematic structure of the supercapacitor. b) CV plots at scan rates of 5–100 $mV s^{-1}$. c) Impedance plot in the frequency range of 0.01 Hz to 100 kHz. Inset: the high-frequency region. d) GCD curves at current densities of 0.25–2.5 $A g^{-1}$. e) Specific capacitance of the supercapacitor at varied GCD current densities. f) Capacitance retention during GCD cyclic tests at a current density of 2.5 $A g^{-1}$. g) CV plots of the supercapacitor at a scan rate of 10 $mV s^{-1}$ under different bending angles. Inset: the definition of bending angle. h) Capacitance retention of the supercapacitor after mechanical folding cycles. Inset: the supercapacitor under the mechanical folding test.

not degrade its electrochemical performance. The CV curves obtained at various bending angles of 0°, 90°, and 180° coincide with each other (Figure 4g), which demonstrates the excellent flexibility of this supercapacitor. After 1000 cycles of mechanical folding, the specific capacitance of this supercapacitor retains 100% of its initial value (Figure 4h), which proves the great mechanical robustness of this supercapacitor. To test the lifetime stability of the PPH-based supercapacitor, its electrochemical performances were measured 1 week and 7 weeks after fabrication. The CV and GCD curves show that the capacitive behavior was well retained (Figure S15). Based on GCD data, the specific capacitance of this supercapacitor showed a decay of 2.4% after 1 week, and a decay of 8.5% after 7 weeks. The specific capacitance based on CV data showed a decay of 3.8% after 1 week, and a decay of 7.1% after 7 weeks, similar to the result based on GCD data. These results demonstrate that the PPH-based supercapacitor is fairly stable, comparable to other flexible supercapacitors.[39,41]

In summary, a supramolecular strategy of crosslinking rigid and soft polymers through dynamic bonds has been developed to prepare a conductive hydrogel with excellent mechanical and electrochemical properties. With a small percentage of boronic acid groups on PANI as crosslink sites, PANI and PVA assemble to form a strong and robust conductive hydrogel with mesoporous structure, which facilitates fast charge transfer and mass transportation within the hydrogel. In PPH, PANI provides fast and reversible charge storage with a high specific capacitance and good chemical stability, while PVA enables the hydrogel with superior mechanical properties. Therefore, PPH can retain its high capacitance despite mechanical deformation or the repeated swelling and shrinking during intensive charge–discharge cyclic processes. Based on this strong, robust, and active PPH material, a flexible solid-state supercapacitor was fabricated, exhibiting high specific capacitance, good cyclic stability and mechanical durability. These outstanding properties enable the PPH-based supercapacitor as a promising power device for flexible electronics. Beyond flexible supercapacitors, the supramolecular strategy of making strong and robust conductive hydrogels based on supramolecular assembly would be a useful approach for other soft matter systems.

Acknowledgements

This work was supported by the National Natural Science Foundation of China (21474094, 81401531), the Natural Science Foundation of Anhui Province (1508085QH154), and the Fundamental Research Funds for the Central Universities (WK2060190044).

Keywords: bioinspired functional materials · conductive polymers · supercapacitors · hydrogels · supramolecular assembly

How to cite: *Angew. Chem. Int. Ed.* **2016**, *55*, 9196–9201
Angew. Chem. **2016**, *128*, 9342–9347

[1] a) G. Zhou, F. Li, H.-M. Cheng, *Energy Environ. Sci.* **2014**, *7*, 1307–1338; b) J. A. Rogers, Y. Huang, *Proc. Natl. Acad. Sci. USA* **2009**, *106*, 10875–10876.
[2] P. Simon, Y. Gogotsi, *Nat. Mater.* **2008**, *7*, 845–854.
[3] a) F. Liu, S. Song, D. Xue, H. Zhang, *Adv. Mater.* **2012**, *24*, 1089–1094; b) Y. N. Meng, Y. Zhao, C. G. Hu, H. H. Cheng, Y. Hu, Z. P. Zhang, G. Q. Shi, L. T. Qu, *Adv. Mater.* **2013**, *25*, 2326–2331; c) T. Chen, R. Hao, H. Peng, L. Dai, *Angew. Chem. Int. Ed.* **2015**, *54*, 618–622; *Angew. Chem.* **2015**, *127*, 628–632.
[4] M. B. Sassin, C. N. Chervin, D. R. Rolison, J. W. Long, *Acc. Chem. Res.* **2012**, *45*, 1062–1074.
[5] T. Liu, L. Finn, M. Yu, H. Wang, T. Zhai, X. Lu, Y. Tong, Y. Li, *Nano Lett.* **2014**, *14*, 2522–2527.
[6] a) X. Xiao, X. Peng, H. Jin, T. Li, C. Zhang, B. Gao, B. Hu, K. Huo, J. Zhou, *Adv. Mater.* **2013**, *25*, 5091–5097; b) A. Sumboja, C. Y. Foo, X. Wang, P. S. Lee, *Adv. Mater.* **2013**, *25*, 2809–2815.
[7] Z. Yang, J. Deng, X. Chen, J. Ren, H. Peng, *Angew. Chem. Int. Ed.* **2013**, *52*, 13453–13457; *Angew. Chem.* **2013**, *125*, 13695–13699.
[8] a) C. Yu, C. Masarapu, J. Rong, B. Wei, H. Jiang, *Adv. Mater.* **2009**, *21*, 4793; b) X. Li, T. Gu, B. Wei, *Nano Lett.* **2012**, *12*, 6366–6371; c) Z. Niu, H. Dong, B. Zhu, J. Li, H. H. Hng, W. Zhou, X. Chen, S. Xie, *Adv. Mater.* **2013**, *25*, 1058–1064.
[9] L. Hu, M. Pasta, F. L. Mantia, L. Cui, S. Jeong, H. D. Deshazer, J. W. Choi, S. M. Han, Y. Cui, *Nano Lett.* **2010**, *10*, 708–714.
[10] D. Son, J. Lee, S. Qiao, R. Ghaffari, J. Kim, J. E. Lee, C. Song, S. J. Kim, D. J. Lee, S. W. Jun, *Nat. Nanotechnol.* **2014**, *9*, 397–404.
[11] S. Ghosh, O. Inganäs, *Adv. Mater.* **1999**, *11*, 1214–1218.
[12] a) L. Pan, G. Yu, D. Zhai, H. R. Lee, W. Zhao, N. Liu, H. Wang, B. C.-K. Tee, Y. Shi, Y. Cui, *Proc. Natl. Acad. Sci. USA* **2012**, *109*, 9287–9292; b) H. Wu, G. Yu, L. Pan, N. Liu, M. T. McDowell, Z. Bao, Y. Cui, *Nat. Commun.* **2013**, DOI: 10.1038/ncomms2941; c) K. Wang, X. Zhang, C. Li, X. Sun, Q. Meng, Y. Ma, Z. Wei, *Adv. Mater.* **2015**, *27*, 7451–7457.
[13] Y. Shi, L. Pan, B. Liu, Y. Wang, Y. Cui, Z. Bao, G. Yu, *J. Mater. Chem. A* **2014**, *2*, 6086–6091.
[14] S. Naficy, J. M. Razal, G. M. Spinks, G. G. Wallace, P. G. Whitten, *Chem. Mater.* **2012**, *24*, 3425–3433.
[15] K. Wang, X. Zhang, C. Li, H. Zhang, X. Sun, N. Xu, Y. Ma, *J. Mater. Chem. A* **2014**, *2*, 19726–19732.
[16] M. Ma, L. Guo, D. G. Anderson, R. Langer, *Science* **2013**, *339*, 186–189.
[17] L. Guo, M. Ma, N. Zhang, R. Langer, D. G. Anderson, *Adv. Mater.* **2014**, *26*, 1427–1433.
[18] Y. Guan, Y. Zhang, *Chem. Soc. Rev.* **2013**, *42*, 8106–8121.
[19] E. Pringsheim, E. Terpetschnig, S. A. Piletsky, O. S. Wolfbeis, *Adv. Mater.* **1999**, *11*, 865–868.
[20] a) T.-S. Tsai, V. Pillay, Y. E. Choonara, L. C. du Toit, G. Modi, D. Naidoo, P. Kumar, *Polymers* **2011**, *3*, 150–172; b) C. Dispenza, M. Leone, C. Lo Presti, F. Librizzi, V. Vetri, G. Spadarol, *Macromol. Symp.* **2007**, *247*, 303–310.
[21] a) S. Adhikari, P. Banerji, *Synth. Met.* **2009**, *159*, 2519–2524; b) A. K. Bajpai, J. Bajpai, S. N. Soni, *J. Macromol. Sci. Pure Appl. Chem.* **2009**, *46*, 774–782.
[22] C. Dispenza, G. Fiandaca, C. Lo Presti, S. Piazza, G. Spadaro, *Radiat. Phys. Chem.* **2007**, *76*, 1371–1375.
[23] J. Xu, K. Wang, S.-Z. Zu, B.-H. Han, Z. Wei, *ACS Nano* **2010**, *4*, 5019–5026.
[24] X. Tang, S. Alavi, *Carbohydr. Polym.* **2011**, *85*, 7–16.
[25] a) J. Huang, R. B. Kaner, *J. Am. Chem. Soc.* **2004**, *126*, 851–855; b) M. R. Gizdavic-Nikolaidis, M. Jevremovic, D. R. Stanisavljev, Z. D. Zujovic, *J. Phys. Chem. C* **2012**, *116*, 3235–3241.
[26] a) L. Chen, B. Kim, M. Nishino, J. P. Gong, Y. Osada, *Macromolecules* **2000**, *33*, 1232–1236; b) Y. Xia, H. Zhu, *Soft Matter* **2011**, *7*, 9388–9393.

[27] R. Ricciardi, F. Auriemma, C. Gaillet, C. De Rosa, F. Lauprêtre, *Macromolecules* **2004**, *37*, 9510 – 9516.
[28] D. Liu, J. Kang, M. Xiang, Y. Cao, *J. Polym. Res.* **2013**, *20*, 939—946.
[29] Y. Okumura, K. Ito, *Adv. Mater.* **2001**, *13*, 485 – 487.
[30] K. Haraguchi, T. Takehisa, *Adv. Mater.* **2002**, *14*, 1120.
[31] J. P. Gong, Y. Katsuyama, T. Kurokawa, Y. Osada, *Adv. Mater.* **2003**, *15*, 1155 – 1158.
[32] M. Malkoch, R. Vestberg, N. Gupta, L. Mespouille, P. Dubois, A. F. Mason, J. L. Hedrick, Q. Liao, C. W. Frank, K. Kingsbury, *Chem. Commun.* **2006**, 2774 – 2776.
[33] S. Sasaki, S. Koga, *J. Phys. Chem. B* **2002**, *106*, 11893 – 11897.
[34] T. Huang, H. Xu, K. Jiao, L. Zhu, H. R. Brown, H. Wang, *Adv. Mater.* **2007**, *19*, 1622 – 1626.
[35] Q. Wu, Y. Xu, Z. Yao, A. Liu, G. Shi, *ACS Nano* **2010**, *4*, 1963 – 1970.
[36] R. Kötz, M. Carlen, *Electrochim. Acta* **2000**, *45*, 2483 – 2498.
[37] a) H. Li, J. Wang, Q. Chu, Z. Wang, F. Zhang, S. Wang, *J. Power Sources* **2009**, *190*, 578 – 586; b) Y. Yan, Q. Cheng, G. Wang, C. Li, *J. Power Sources* **2011**, *196*, 7835 – 7840; c) F. Xu, G. Zheng, D. Wu, Y. Liang, Z. Li, R. Fu, *Phys. Chem. Chem. Phys.* **2010**, *12*, 3270 – 3275; d) K. S. Ryu, K. M. Kim, N.-G. Park, Y. J. Park, S. H. Chang, *J. Power Sources* **2002**, *103*, 305 – 309.
[38] T. Kobayashi, H. Yoneyama, H. Tamura, *J. Electroanal. Chem.* **1984**, *177*, 281 – 291.
[39] C. Meng, C. Liu, L. Chen, C. Hu, S. Fan, *Nano Lett.* **2010**, *10*, 4025 – 4031.
[40] a) G. Wang, H. Wang, X. Lu, Y. Ling, M. Yu, T. Zhai, Y. Tong, Y. Li, *Adv. Mater.* **2014**, *26*, 2676 – 2682; b) L. Yuan, X.-H. Lu, X. Xiao, T. Zhai, J. Dai, F. Zhang, B. Hu, X. Wang, L. Gong, J. Chen, C. Hu, Y. Tong, J. Zhou, Z. L. Wang, *ACS Nano* **2012**, *6*, 656 – 661; c) X. Lu, G. Wang, T. Zhai, M. Yu, S. Xie, Y. Ling, C. Liang, Y. Tong, Y. Li, *Nano Lett.* **2012**, *12*, 5376 – 5381.
[41] Y. X. Xu, Z. Y. Lin, X. Q. Huang, Y. Liu, Y. Huang, X. F. Duan, *ACS Nano* **2013**, *7*, 4042 – 4049.

Received: April 7, 2016
Revised: May 9, 2016
Published online: June 22, 2016

